Measurement of Mass Flux in Two-Phase Flow Using Combinations of Pitot Tubes and Gamma Densitometers

New experimental data indicate that mass flux in cocurrent gas-liquid flows may be determined by the use of Pitot tubes in conjunction with a local mixture density measurement technique. The data were taken over a wide range of flow regimes in a horizontal pipe and included separated patterns such as stratified and annular flows. Local mixture densities were obtained by a computer-assisted algebraic reconstruction technique that used chordal average densities measured by traversing gamma beam attenuation.

The results extend the applicability of this mass flux measurement technique well beyond the relatively homogeneous, high-pressure, steam-water flow situations originally studied by Banerjee and Nguyen (1977).

K-F F-L HAU

S. BANERJEE

McMaster University
Department of Engineering Physics
Hamilton, Ontario L8S 4M1

SCOPE

The objective was to investigate the performance of Pitot tubes for measuring mass flux over a wide range of two-phase flow regimes, particularly those in which the phases were well separated and moved with substantially different average velocities.

Mass flux measurements are of interest in many industrial and research applications. For example, it is one of the main parameters needed in experiments related to the thermal and hydraulic aspects of reactor safety. Other applications include oil-gas pipelines, geothermal wells and wet steam distribution networks for *in-situ* tar sands extraction. Motivated by the demand for such measurements, extensive work has been done on devices such as orifice and venturi meters, turbine flowmeters, drag screens and disks, and tracer transit time measurement techniques. The state of the art has recently been reviewed by Banerjee and Lahey (1980). All the techniques studied appear to have disadvantages that limit their applicability and none is completely satisfactory. This has led, in part, to the present investigation of Pitot tubes for two-phase mass flux measurements.

Pitot tubes are rugged and relatively simple so that they can be used in adverse environments, like the LOFT (Loss of Fluid Test) reactor under blowdown conditions. On the other hand, their response in two-phase flow is not well understood. Work by Banerjee and Nguyen (1977), Banerjee, et al. (1978) and Heidrick et al. (1978) indicated that a simple response model involving cross-section averaged mixture density could be used to calculate mass flux in high-pressure, high-velocity steam-water flows. The measurements were made in flow regimes that were relatively homogeneous. Questions remained as to the usefulness of the technique in the more separated flows that might occur at lower pressures, higher void fractions and lower velocities.

To clarify the situation, steady-state experiments were done in horizontal air-water flow at low pressure in order to obtain large density and, possibly, large velocity differences between the phases. The air and water superficial mass fluxes were varied between 0.1 and 22 $kg/m^2 \cdot s$, and between 130 and 1700 $kg/m^2 \cdot s$, respectively. This resulted in measurements being made in annular, slug annular, slug, plug and wavy stratified flows.

To interpret Pitot tube response in two-phase flows, local mixture densities appeared to be needed, and were calculated by an algebraic reconstruction technique that used chordal averaged values obtained by traversing gamma beam attenuation. Models for Pitot tube response were developed in terms of local mixture mass flux and local mixture density. They were then tested by integrating the mass flux across the flow cross-section and comparing the results with the input mass flux.

CONCLUSIONS AND SIGNIFICANCE

A model for Pitot tube response similar to that for single-phase flow was initially tested; i.e., the local mixture mass flux was calculated as the square root of twice the product of the local mixture density and Pitot impact pressure. The test was carried out by obtaining the local mixture mass flux at many locations at a flow cross-section, integrating over the cross-section to obtain the average mass flux, and then comparing this to the known input mass flux.

The cross-section averaged mass fluxes measured by this method were in good agreement with the input values for the whole range of conditions studied. In addition, the model gave equally good results if the average mixture density measured along horizontal chords was used, in place of the local mixture density, with Pitot tube measurements along the chord. This was significant, because it is relatively easy to measure chordal average mixture densities using gamma beam attenuation.

We also investigated the adequacy of average mass flux predictions using Pitot tube measurements at only a few locations. For our 50-mm I.D. horizontal pipe, four measurements located along a vertical line through the center of the pipe were sufficient. Optimum locations were not sought, since these might vary with flow regime, pipe size and upstream conditions.

Finally, work was done on the use of the algebraic reconstruction technique along with measurements using traversing gamma beams to obtain local mixture densities. Though this development was not the main purpose of the investigation, it

0001-1541-81-4376-0177-$2.00.

proved successful and may be of use in applications where the average phase distribution is needed.

The main conclusion that can be drawn from this and earlier work is that a model for Pitot tube response analogous to that for single-phase flow, gives good predictions of cross-section averaged mass flux.

Ideally, a sufficient number of Pitot tube and local mixture density measurements must be made to get good coverage over the flow cross-section. However, our experiments indicate that relatively few Pitot tube measurements may be used together with the appropriate chordal average mixture densities to predict average mass flux quite well. This is important in applications, because equipment for measuring these quantities are easy to fabricate and install.

INTRODUCTION

Recent advances in two-phase flow measurement techniques have been reviewed by Hewitt and Lovegrove (1976), Brockett et al. (1976), Delhaye (1973), and Banerjee and Lahey (1980). As discussed in these reports, mass flux is one of the parameters of engineering interest, and also one of the most difficult to measure. Limited success has been attained in making such measurements using combinations of instruments to measure mixture density (or void fraction) and flow, together with appropriate response models. For example, multibeam gamma densitometers and turbine flowmeters or drag disks may be used as described by Banerjee and Lahey. Pitot tubes have also been considered for measuring flow because of their ruggedness and good performance in high-pressure, high-temperature environments (Banerjee et al., 1978).

Banerjee and Lahey (1980) have reviewed the state of the art with regard to mass flux measurements by Pitot tubes in two-phase flow. Suffice it to say that the lines between the Pitot tubes and pressure transducers should be liquid-filled to obtain good frequency response and that the simplest model for local mass flux results in:

$$G_{\text{local}} = \rho_m v_{\text{local}} = \sqrt{2\rho_m \Delta P_i} \qquad (1)$$

It is possible to check how well Eq. 1 works by integrating over the flow cross-section to obtain the average mass flux and comparing with input values. This is done in later sections.

Previous experiments by Banerjee et al. (1978) and Heidrick et al. (1978) suggested that Pitot tube-mixture density measurements could be used to predict mass fluxes in relatively homogeneous flows. They corrected for velocity profile effects by using a calibration factor obtained in single-phase flow experiments. However, doubts have remained as to the usefulness of the technique in separated flows, e.g., stratified or annular. The work reported here was, therefore, to investigate the performance of such combined measurements over a wide range of flow regimes. The effects of pressure, pipe diameter and upstream conditions were not part of this investigation. This was because the conditions chosen (low-pressure air-water in 50.8-mm I.D. pipe) were considered to be sufficient to give well separated flows. If the technique worked in these situations as well as in relatively homogeneous flows, it would be reliable over a wide range of conditions.

EXPERIMENTAL APPARATUS

The overall arrangement of the experimental rig is shown schematically in Figure 1. Air and water passed through a Y-shaped mixer, and the two-phase mixture then flowed through a 4.27 m long, 50.8 mm I.D. Lucite pipe into a separating tank where the air was discharged to atmosphere and the water was recirculated. The volumetric flow rates of air and water were measured by three turbine flow meters which had been calibrated to within an accuracy of ±15%, ±5% and ±15%, respectively (with 98% confidence limits).

γ-Densitometer

A γ-densitometer consisting of 100 m Ci Pu 238, a collimator and a collimated sodium iodide scintillation detector with associated electronics was located at 3.58 m (approximately 70 diameters) downstream from the entrance. It was mounted on a

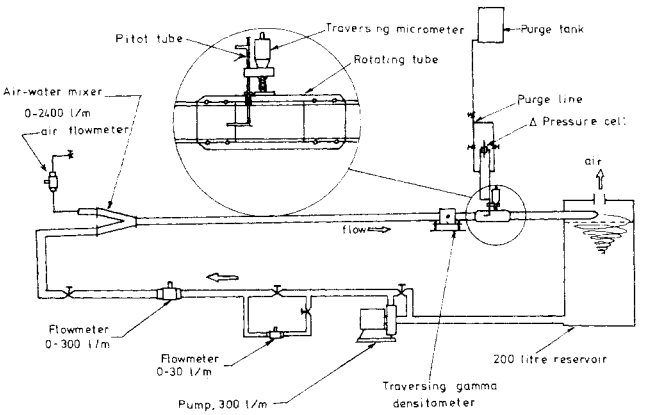

Figure 1. Two-phase flow loop.

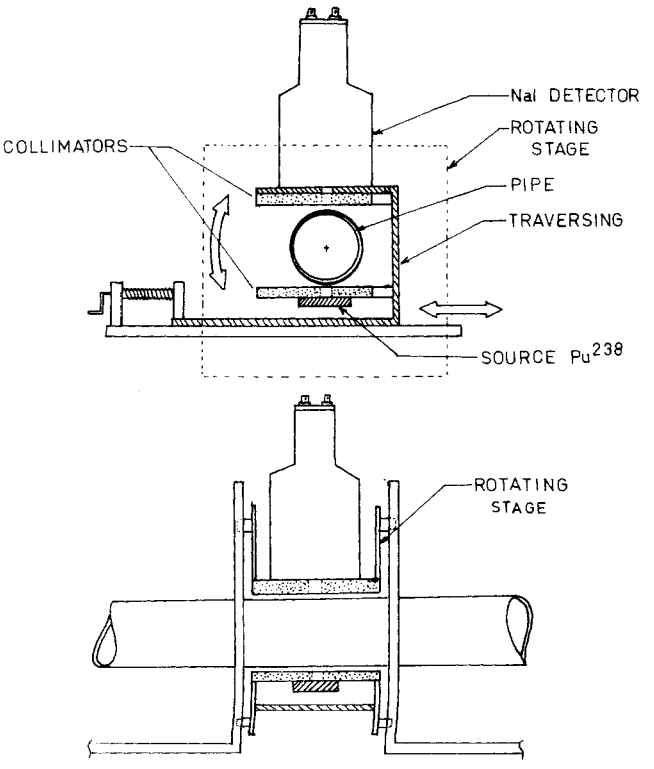

Figure 2. Traversing γ-densitometer.

traversing mechanism such that the void fraction could be scanned along vertical chords, as well as along horizontal chords. The mechanism consisted of two parts: one part allowed the γ-densitometer to be moved in the direction perpendicular to the γ-beam, and the other part allowed the γ-densitometer to be rotated around the pipe axis. A schematic drawing of this traversing mechanism which is self-explanatory is shown in Figure 2.

The electronics associated with γ attenuation measurements are shown schematically in Figure 3. Power for the detector was supplied from a Harshaw high-voltage D.C. power supply. The signal from the output of the photomultiplier tube of the detector was fed into a single module preamplifier/amplifier/single channel analyzer. The single channel analyzer produced an output pulse only when the amplifier output pulse fell within a specified energy window, and consequently background radiation and noise could be reduced to a minimum. The signal from the output of the analyzer was fed to a frequency/voltage converter and then to a log-amplifier. The output voltage from the log-amplifier was then integrated by an integrator to give time mean values. An integration period of 60 seconds was found to be sufficient for most applications. The time averaged chordal void fraction $\bar{\alpha}_i$ was then calculated using the following equation.

$$\bar{\alpha}_i = \frac{\ln I_x - \ln I_l}{\ln I_g - \ln I_l} \tag{2}$$

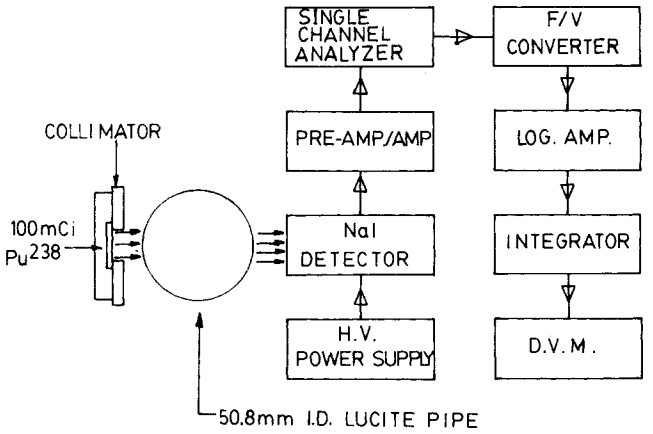

Figure 3. Electronic circuit for γ-densitometer.

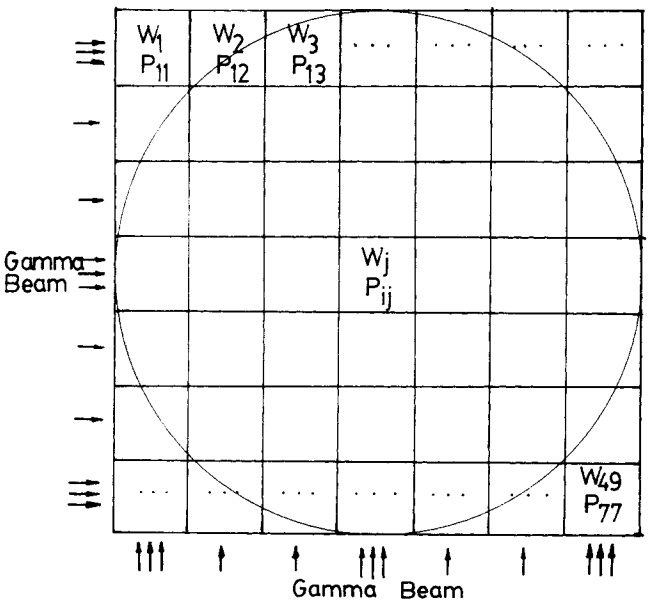

Figure 4. Reconstruction model for a two-dimensional void distribution.

This equation is expected to be accurate only when the gas-liquid layers cross the gamma beam. This occurs in most practical situations except for stratified flow, for which the gas-liquid layers may be parallel to horizontal gamma beams. This aspect will be discussed later.

Pitot Tube Assembly

A Pitot tube was installed 0.3 meter downstream from the location of the γ-densitometer. It was mounted on a traversing micrometer which was permanently fixed onto a spool piece which could be rotated about its axis, Figure 1. This traversing mechanism allowed the Pitot tube to be located in any position within the 50.8-mm I.D. pipe.

A Validyne differential pressure transducer with either a 7-kPa or a 1.4-kPa diaphragm was used to measure the difference in pressure between the impact head and the static head for the Pitot tube. To assure accuracy the connecting lines between the Pitot tube and the transducer were kept liquid filled by using a metered water purge.

The signal from the output of the pressure transducer was fed to a demodulator and then to an integrator or through a square root operator and then to an integrator. The time mean value of the differential pressure, $\langle \Delta P(t) \rangle$, and the time mean value of the square root of the differential pressure $\langle \sqrt{\Delta P(t)} \rangle$ could, therefore, be obtained.

INTERPRETATION OF EXPERIMENTAL DATA

Calculation of Mass Flux

To calculate the local mass flux in a two-phase mixture from Pitot tube measurements, it is necessary to model the Pitot tube response in terms of impact pressure to a given mass flux and mixture density at the probe tip. The simplest model is to assume that the mass flux at any location, G_{ij}, is given by the usual single-phase Pitot equation,

$$G_{ij}(t) = \sqrt{2\rho_{ij}(t)\Delta P_{ij}(t)} \tag{3}$$

This procedure is open to question since different momentum transfer factors may obtain for gas and liquid (Anderson and Mantzourauis, 1960). Therefore, Eq. 3 must be regarded only as a possible model and its accuracy determined by comparison with experimental data. The time averaged local mass flux $\langle G_{ij} \rangle$ is then:

$$\langle G_{ij} \rangle = \langle \sqrt{2\rho_{ij}(t)\Delta P_{ij}(t)} \rangle \tag{4}$$

At present, it does not appear to be possible to measure the instantaneous local fluid density just in front of the Pitot tube without disturbing the flow substantially. It is, therefore, further assumed that the instantaneous fluid density can be replaced by its time mean value in Eq. 3.

For the initial set of experiments, we measured chordal averaged void fractions and did not reconstruct the mixture density distribution. In order to proceed, we had to assume that the mixture density was uniform along a horizontal chord. The (time averaged) local mass flux based on these assumptions could then be calculated from the measured time averaged chordal void fractions and the time mean value of the square root of the differential pressure of the Pitot tube,

$$\langle G_{ij} \rangle = \sqrt{2[\rho_l(1 - \bar{\alpha}_i) + \rho_g \bar{\alpha}_i]} \times \langle \sqrt{\Delta P_{ij}(t)} \rangle \tag{5}$$

In the later set of experiments, local time averaged void fractions were obtained by using an algebraic reconstruction technique (ART) to unfold the mixture density distribution from horizontal and vertical chordal void fraction measurements.

The computed time averaged local void fractions α_{ij} were then used for calculating the local time averaged mass flux instead of the chordal void fraction in Eq. 5. The local mass flux was then:

$$\langle G_{ij} \rangle = \sqrt{2[\rho_l(1 - \alpha_{ij}) + \rho_g \alpha_{ij}]} \times \langle \sqrt{\Delta P_{ij}(t)} \rangle \tag{6}$$

Note that there is some ambiguity in the manner in which the average impact pressure should be determined. The time averaged local mass flux could also be determined by equations of the form;

$$\langle G_{ij} \rangle = \sqrt{2[\rho_1(1 - \bar{\alpha}_i) + \rho_g \bar{\alpha}_i]} \times \sqrt{\langle \Delta P_{ij}(t) \rangle} \quad (7)$$

and

$$\langle G_{ij} \rangle = \sqrt{2[\rho_1(1 - \alpha_{ij}) + \rho_g \alpha_{ij}]} \times \sqrt{\langle \Delta P_{ij}(t) \rangle} \quad (8)$$

If the mixture density was truly constant at a given location, Eqs. 5 and 6 are obviously the more correct form. However, the impact pressure ΔP can be expected to increase and decrease with the fluctuating mixture density. If these fluctuations in impact pressure were roughly proportional to the fluctuations in mixture density, Eqs. 7 and 8 are more correct.

The true situation lies somewhere in between, because the impact pressure may fluctuate to some extent due to fluctuations in local velocity. There is no way of accounting for this effect accurately at present, since we cannot measure the instantaneous local density. Therefore, both Eqs. 5 and 6 and Eqs. 7 and 8 have been used in our analysis with the expectation that the actual situation is in between these.

The average chordal mass fluxes were calculated from the measured local mass fluxes, which in turn were obtained either from Eqs. 5 and 6 or from Eqs. 7 and 8. The chordal averages were obtained by integration assuming a one-seventh power law velocity profile very close to the wall. The average mass flux across the pipe was then calculated by integrating the average chordal mass fluxes. The integrations were done by Simpson's rule.

Reconstruction of Local Mixture Density Distribution

An algebraic reconstruction technique, first introduced apparently by Gordon et al. (1970) to reconstruct the form of a 250 Å ribosome, was used to determine the local mixture density for void fraction distribution. Gordon et al.'s original algorithm, along with improved versions, have been reviewed by Herman et al. (1973).

More recently, Zakaib et al. (1978) have applied the algebraic reconstruction technique in an investigation of void fraction distribution using thermal neutron transmission measurements. In the present study, a similar method was, therefore, used to reconstruct two-dimensional local void distribution over a 7×7 grid from 14 gamma transmission measurements which gave chordal average mixture densities. The 14 measurements were made over two projections, one set horizontal and the other vertical.

We will briefly review the algebraic reconstruction technique as used in our code. Let W_j be the local liquid fraction (i.e., $W_j = 1 - \alpha_j$), and P_{ij} be the fraction of area of the jth square in which it is intersected by the ith ray, Figure 4. The measured chordal liquid fraction R_i (i.e., $R_i = 1 - \bar{\alpha}_i$) at ith chord can be expressed in terms of W_j and P_{ij} as:

$$R_i = \frac{1}{\sum_{j=1}^{n^2} P_{ij}} \sum_{j=1}^{n^2} P_{ij} W_j \quad (9)$$

Eq. 9 can also be written in a matrix form,

$$[P]^{m \times n^2}[W]^{n^2} = [N_p \cdot R]^m \quad (10)$$

where

$$(N_p)_i = \sum_{j=1}^{n^2} P_{ij}$$

and

$$m << n^2$$

$$0 \le W_j \le 1 \text{ for } 1 \le j \le n^2$$

For the present case, m and n in Eq. 10 equal 14 and 7, respectively.

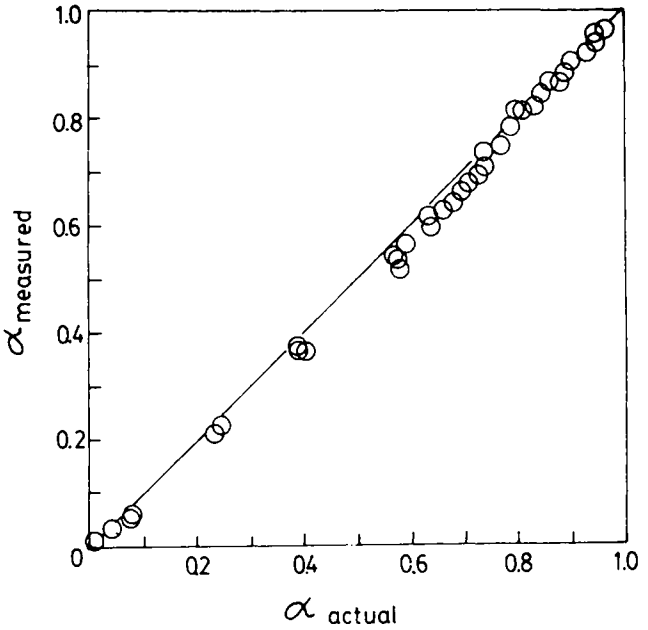

Figure 5. Measured chordal voids vs. actual values—when the γ-beam is perpendicular to Lucite layers.

The algebraic reconstruction technique (Gordon et al., 1970) is basically used for solving a set of linear equations which are highly underdetermined, as shown in Eq. 10. It is an iterative method. Let W_j^q denote the estimated value of W_j after q iterative steps, W_j^{q+1} can be calculated from an equation.

$$W_j^{q+1} = W_j^q + P_{ij} \times (R_i - R_i^q) \quad (11)$$

where

$$R_i^q = \sum_{j=1}^{n^2} P_{ij} W_j^q \Big/ \sum_{j=1}^{n^2} P_{ij}$$

$$W_j^{q+1} = \begin{cases} W_j^{q+1} & \text{if } 0 \le W_j^{q+1} \le 1 \\ 0 & \text{if } W_j^{q+1} < 0 \\ 1 & \text{if } W_j^{q+1} > 1 \end{cases}$$

The initial guess for W_j is set to be the average liquid fraction across the pipe $\bar{W}$, i.e.,

$$W_j^0 = \bar{W} = 1 - \bar{\alpha}$$

Herman et al. (1973) found empirically that the iterative algorithm had converged to the solution when a criterion based on the change of variance was less than one percent, i.e.,

$$|V^{q+1} - V^q| < V^q/100 \quad (12)$$

where

$$V^q = \sum_{j=1}^{n^2} (W_j^q - \bar{W})^2$$

This criterion was chosen for the present study.

EXPERIMENTAL RESULTS AND DISCUSSION

Preliminary Tests

A series of tests was done in a single-phase flow to test the behavior of the system and the accuracy of the experimental technique.

The calculated mass fluxes from the Pitot tube measurements agreed (within ±6%) with the input mass flux measured by calibrated turbine flow meters. For the single-phase runs, the void fraction was, of course, always zero and the pressure fluctuations at the Pitot tube were quite small; so, Eqs. 8 to 11 gave essentially the same results.

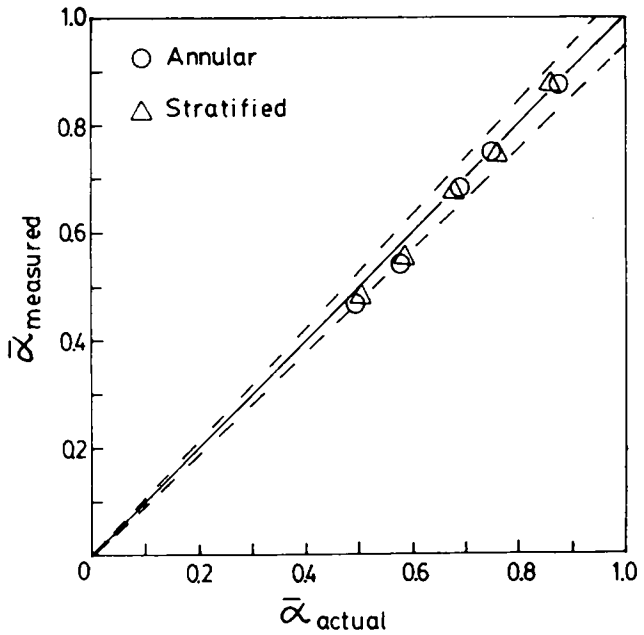

Figure 6. Measured cross-section averaged void fractions vs. actual values.

These experiments indicated that all components of the system to be used for the two-phase flow experiments, except for the γ beam attenuation system, were working well. Separate experiments were done to check the gamma system.

Calibration of γ-Densitometer

As mentioned previously, Eq. 2 is not always accurate for calculation of chordal averaged void fractions; therefore, calibration curves were obtained with Lucite mock-ups, which simulated annular and stratified flows. The range of void fractions selected for study were from 0.50 to 0.87 for annular flow and from 0.50 to 0.85 for stratified flow.

For the cases where the γ-beam was perpendicular to the Lucite layer, the measured void fractions agreed very well with actual values for $\alpha > 0.8$, but were generally lower than actual values for $\alpha < 0.8$ as shown in Figure 5. The differences (in absolute value) increased to a maximum ($\sim$0.08) at $\alpha \approx 0.6$ and decreased as $\alpha < 0.6$.

For the cases where the γ-beam was parallel to the Lucite layer, the measured α calculated from Eq. 2 was different from actual values. This is to be expected since Eq. 2 does not really apply in this case. For example, it has been suggested by Patrick and Swanson (1958) that when the liquid and gas exist in layers parallel to the beam, the void fraction should be calculated by an equation of the form,

$$\alpha_i = \frac{I_x - I_l}{I_g - I_l} \tag{13}$$

These remarks apply only to the chordal averaged void fraction which is of importance in interpreting the Pitot tube readings. The cross-section averaged void fractions (based on Eq. 2) and the actual values are compared in Figure 6. The measured cross-section averaged void fractions agreed well (within $\pm$15%) with their actual values over the experimental range ($0.5 < \alpha < 0.9$).

For simplicity, Eq. 2 was used for calculating the chordal void fraction throughout tests. However, corrected values based on calibration curves were also used in some cases to determine differences. It appeared that the differences between the results from the approximate equation and the calibration curve were generally rather small as discussed later.

Verification of the Algebraic Reconstruction Technique

To test the applicability and the accuracy of the ART for reconstructing the local void distribution from 14 horizontal and vertical chordal void measurements, five sets of tests were performed with digital models to simulate various hypothetical local void distributions over 7 × 7 grids. Horizontal and vertical chordal void fractions were evaluated from the hypothetical local void distributions and fed into the ART computer program to reconstruct the local void distributions. Good agreement was obtained between the hypothetical local void distributions and the computed void distributions as shown in Figure 7(a, b).

The computer program was also checked out by performing a series of experiments with Lucite mockups of various shapes to

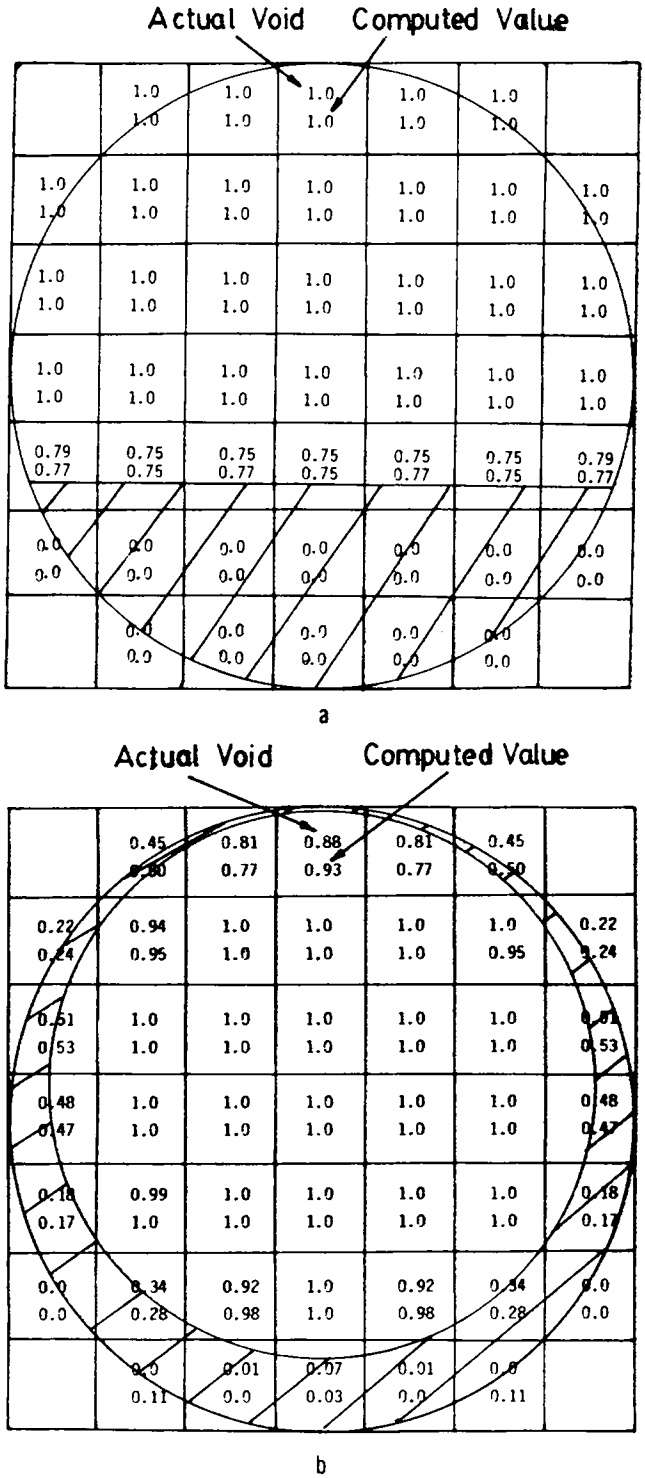

Figure 7. Test of ART computer program with hypothetical void fraction data.
a. Annular flow.
b. Stratified flow.

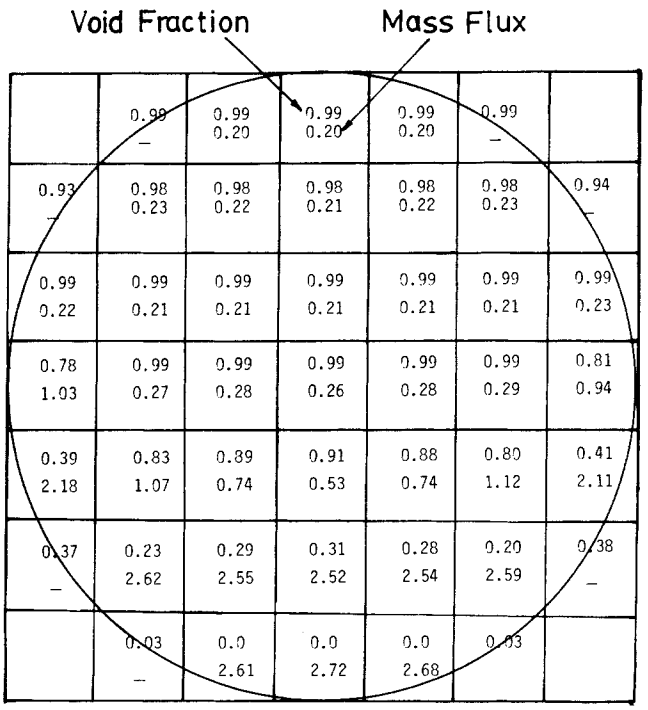

Figure 8. Local void fraction and normalized mass flux distributions for annular flow.

simulate different water distributions. Horizontal and vertical chordal void fractions were measured by a traversing gamma-densitometer. The void distributions of the Lucite mockups computed from the measured horizontal and vertical chordal void fractions by the ART computer program also agreed quite well with the actual void distributions.

As expected, the void fractions near the wall region were generally lower than those further from the wall for annular, slug, and plug flows, and tended to all water at the very bottom. For the wavy stratified flow, the void fraction was one in the upper half of the pipe and tended to zero in the bottom half of the pipe.

In general, the local mass fluxes seemed to be quite uniform over almost the whole region of each horizontal chord except for some regions near the wall in annular flow, Figure 8, where the void fraction was lower, and a higher mass flux was, therefore, obtained as a consequence of a higher value of the product of the fluid density and the flow velocity. Certainly, the mass flux should decrease sharply in the region very near the wall and reach zero at the wall, but it is not possible to measure this due to finite probe size.

Figure 9 shows that in all cases the chordal mass fluxes in the bottom half of the pipe are much higher than those in the upper half of the pipe, especially in the cases of wavy stratified, annular and slug flows. For the plug flow, the chordal mass fluxes are more uniform compared to the other three flow regimes.

Cross-Section Averaged Mass Flux

The cross-section averaged mass flux was calculated from the distribution of local mass fluxes by integration as described previously.

Comparisons of the measured cross-section averaged mass fluxes and the input mass fluxes are shown in Figure 10. Different symbols for the experimental data points shown in this figure represent different flow patterns. For the high water flow range, it seems that the calculated mass fluxes from Eq. 5 (the empty symbols) are generally 0 to 10% lower than the input mass fluxes. On the other hand, Eq. 7 (the dark symbols) seems to overestimate the mass flux (by up to 13%). As discussed previously, neither Eq. 5 nor 7 is correct in the case of fluctuating densities—the real situation lies somewhere in between. Therefore, these results are consistent with what is expected.

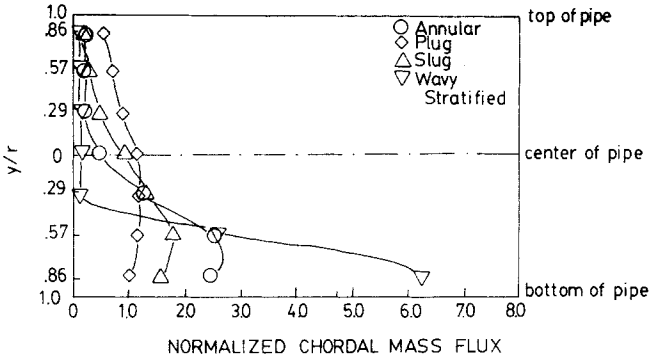

Figure 9. Distributions of normalized chordal mass fluxes (y is the distance from the center of the pipe in the vertical plane).

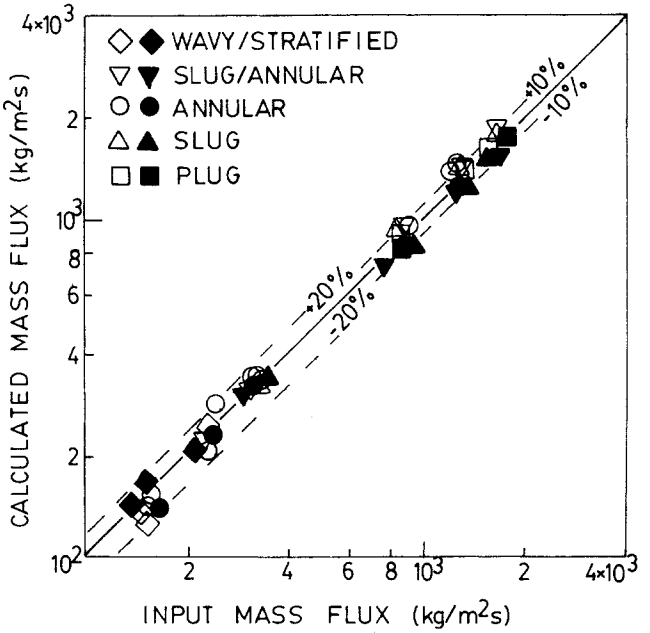

Figure 10. Comparison of measured mass fluxes and input mass fluxes—measured mass fluxes were calculated from Eqs. 5 and 6.

For the low water flow range (< 800 kg/m$^2 \cdot$ s), the calculated mass fluxes from Eqs. 5 and 7 agree quite well among themselves. The difference in the results for the high- and low-water flow ranges is much likely due to the different relative magnitude of the pressure fluctuations occurring in the high- and low-water flow ranges. In any case, either equation appears to be reasonably accurate, within $\pm 10\%$ for the high mass fluxes and $\pm 20\%$ for the low mass fluxes, in predicting mass flux over the whole range of experiments.

It is important to remember that both Eqs. 5 and 7 were based on the assumption that the fluid density was homogeneous across the chord. Obviously, it is unlikely to be true in the actual case. However, the deviation of the calculated mass fluxes arising from this effect was found to be quite small, when local mixture densities (or void fractions) were used.

Local void distributions were obtained from the measured horizontal and vertical void fractions by using the ART algorithm; hence, the local mass fluxes could be calculated from Eqs. 6 and 8. It was found that the differences between the cross-section averaged mass fluxes, which were calculated from Eqs. 5 and 7 (i.e., based on an assumption that the fluid density is homogeneous across horizontal chords) and from Eqs. 6 and 8 (i.e., based on the computed local fluid densities) respectively were quite small (up to 5%). This is to be expected since the void distribution is quite uniform along horizontal chords except very near the wall and in annular flow. The cross-section averaged

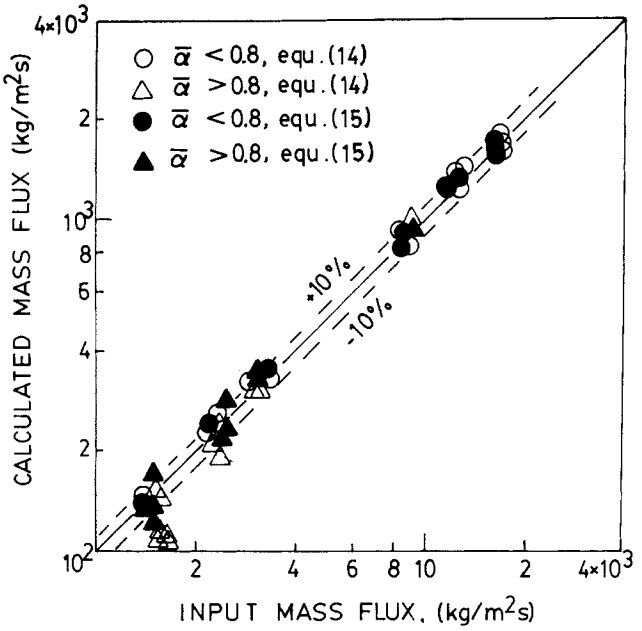

Figure 11. Mass fluxes predicted from three and four local measurements (○ △ three local measurements, ● ▲ four local measurements).

mass flux calculated from the local void fractions should have a somewhat lower value because of this affect, as they indeed do.

In addition, comparisons of the mass fluxes between those calculated from the measured chordal $\bar{\alpha}_i$ based on Eq. 2 and those calculated from the corrected values of the chordal $\bar{\alpha}_i$ accounting for the inaccuracies in Eq. 2 also show that there were only small differences between the two (less than 3%) over the whole range of flow patterns, except for wavy stratified flows. In this case, the values calculated from the corrected values of the chordal void fraction had a larger value (up to 16%) than those calculated from the uncorrected chordal void fractions. This is due to the lower values of the corrected chordal void fraction (i.e., larger mixture density).

However, it was found that the deviation of calculated cross-section averaged mass fluxes arising from the local void distribution effect and the uncertainties in Eq. 2 for void fraction calculations, is small over the whole range of flow patterns. This result is significant as it indicates that the cross-section averaged mass flux may be obtained quite accurately from the local Pitot tube measurements and the measured chordal fluid densities. This is not a general conclusion, but applies only for the conditions studied in our experiments, i.e., horizontal flows far from bends such that the main void distribution is in the vertical direction. If there is a bend near the measurement location, the void distribution may be nonsymmetric and local values would be necessary.

Effect of Reducing the Number of Local Measurements

For practical purposes, it is of interest to find locations for a small number of Pitot tubes and γ-beam measurements that would still result in good accuracy for cross-section averaged mass flux over a range of flow regimes.

From the distributions of the local mass fluxes (those based on the chordal mixture densities), it seems that a local measurement near the central region of a horizontal chord is good enough to predict the (horizontal) chordal mass flux in most flow regimes due to the uniformity of the local mass fluxes along the chord. It was found that the cross-section averaged mass flux could be obtained from only three Pitot tubes and chordal γ-densitometer measurements. The Pitot tubes were positioned in a vertical line, one at the center of the pipe, one at 0.286 diameter above the center and one at 0.286 diameter below the center. These positions lead to each Pitot tube covering roughly the same amount of flow area in horizontal segments. The average mass flux was calculated by an equation of the form

$$\bar{G} = \frac{G_2 + G_4 + G_6}{3} \times C_1 \qquad (14)$$

where C_1 is obtained from single-phase calibration measurements. This is similar to the original procedure used by Banerjee et al. (1978). The value of C_1 was calculated from the single-phase (all water) measurements to be 0.85.

Figure 11 shows the comparison of the calculated mass fluxes from Eq. 14 and the input mass fluxes. It can be seen that the agreement between the two is quite good for the cases when the cross-section averaged void fraction is less than 0.8. But for the cases $\alpha > 0.8$, the calculated mass fluxes were generally lower than the input mass fluxes. This can be explained by the fact that the flow was horizontally stratified and the Pitot tube in the bottom half of the pipe was above much of the liquid flow region for these cases. Therefore, positioning three Pitot tubes in a vertical line such that they cover roughly the same area in horizontal segments is not sufficient for separate flows with $\alpha > 0.8$.

Taking this into consideration, a fourth measurement near the bottom wall (at 0.429 diameter below the center of the pipe), in addition to the three measurements, appears to be needed. The simple procedure is to area weight the bottom two measurements and an equation for the cross-section averaged mass flux of the form:

$$\bar{G} = \frac{G_2 + G_4 + G_6'}{3} \times C_1 \qquad (15)$$

where

$$G_6' = (1 - C_2)G_6 + C_2G_7$$

$C_1 = 0.85$ is the original single phase calibration constant and C_2 is a constant giving the fraction flow of area covered by the Pitot tube at 7, compared to the total area covered by 6 and 7 in horizontal segments. For the case studied here, $C_2 \sim 0.15$. As can be seen from Figure 10, mass fluxes calculated from Eq. 15 agree quite well with the input mass fluxes even for $\alpha > 0.8$. Therefore, it would probably be desirable to obtain the cross-section averaged mass fluxes from four local measurements rather than three to ensure that all flow regimes are covered.

Future Work

The results obtained in this investigation are encouraging and, combined with previous related work, put the use of Pitot tubes for mass flux measurements in two-phase flow on quite a firm basis. There are some areas in which further experiments would be desirable:

- Measurements in very large horizontal pipes under separated flow conditions. These experiments would increase confidence in the use of Pitot tubes in separated flows. Some experiments are being done in pipes of 0.3556-m nominal diameter at present.
- Checks on whether local mass fluxes are being measured correctly. The results discussed in this paper are for cross-section averaged mass fluxes derived by integrating local values. No direct test of the local measurements was done. Therefore, the model proposed is at best supported by indirect evidence. A technique based on hot film anemometry could possibly be developed and compared with Pitot tube measurements of time averaged local mass flux. Even though hot film anemometry may not be accurate or practical in high pressure and temperature systems, still good agreement between the two techniques would enhance confidence in both.
- The effect of multidimensional flow on Pitot tube measurements. Experiments could be done by repeating those in this paper with Pitot tubes positioned at various angles to the pipe axis. Such experiments are of interest, because Pitot tubes have been suggested for use in two-phase flows that have swirl and large-scale eddy structure. In these situations, the mean velocity vector may not point directly at the Pitot tube.

• Measurements in transients under separated flow conditions. Some measurements of this type are being done using a six Pitot tube "rake" in a large pipe.

ACKNOWLEDGMENT

We would like to thank the Idaho National Engineering Laboratory, Idaho Falls, and Atomic Energy of Canada, Pinawa, Manitoba, for supporting this work. We would also like to acknowledge the assistance provided by Martin Vandenbroek during the experiments.

NOTATION

C_1, C_2 = constants, defined by Eqs. 14 and 15, respectively
G_2, G_4, G_6, G_7 = local mass flux at 0.286 diameter above the center of the pipe, at the center, at 0.286 and 0.429 diameter below the center, respectively
G'_6 = local mass flux, defined by Eq. 15
G_{ij} = local mass flux at location ij
$\overline{G}$ = cross-section averaged mass flux
I_x = measured gamma intensity
I_l, I_g = intensities measured for the cases of the tube full of liquid and gas, respectively
P_{ij} = fraction of area of the jth square in which it is intersected by the ith ray
$\Delta p_{ij}(t)$ = instantaneous differential pressure of the impact head at position ij
R_i = chordal liquid fraction at ith chord
V = velocity
V^q = variance, defined by Eq. 12
W_j = local liquid fraction at position j
$\overline{W}$ = cross-section averaged liquid fraction
α_{ij}, α_j = local void fraction at position ij and j, respectively
$\overline{\alpha}_i$ = chordal void fraction at ith chord
ρ = density
$\rho_{ij}(t)$ = the instantaneous local fluid density at position ij
$\langle\ \rangle$ = time mean value

Subscript

g = gas phase
l = liquid phase
m = mixture

LITERATURE CITED

Anderson, G. H., and B. G. Mantzouranis, "Two-Phase (Gas/Liquid) Flow Phenomena—II Liquid Entrainment," *Chem. Eng. Sci.*, **12**, 233 (1960).

Banerjee, S., and D. M. Nguyen, "Mass Velocity Measurement in Steam-Water Flow by Pitot Tubes," *AIChE J.*, **23**, 385 (1977).

Banerjee, S., T. R. Heidrick, and E. Rhodes, "Development and Calibration of Instruments in Transient Two-Phase Flow," Proceedings of the OECD/CSNI Specialists Meeting on *Transient Two-Phase Flow*, Paris, France (June, 1978).

Banerjee, S., and R. T. Lahey, "Advances in Two-Phase Flow Instrumentation," *Advances in Nuclear Sci. and Tech.*, (1980, in press).

Brockett, G. F., and R. T. Johnson, "Single Phase and Two-Phase Flow Measurement Techniques for Reactor Safety Studies," Electric Power Research Institute Report, *EPRI-ND-195* (1976).

Delhaye, J. M., "Two-Phase Flow Measurements," *Bull. D'Inform. Sci. Tech.*, **197**, S-20 (1963).

Gordon, R., R. Bender, and G. T. Herman, "Algebraic Reconstruction Technique (ART) for Three-Dimensional Electron Microscopy and X-Ray Photography," *J. Theor. Biol.*, **29**, 471 (1970).

Heidrick, T. R., J. R. Saltvold, and S. Banerjee, "Application of a 3-Beam γ-Densitometer to Two-Phase Flow Regime and Density Measurements," *AIChE Symposium Series*, **73**, No. 164, 248 (1978).

Heidrick, T. R., J. R. Saltvold, S. Banerjee, and D. Nguyen, "Cross-Section Averaged Density and Mass Flux Measurements in Two-Phase Flow Through Pipes," *Measurements in Polyphase Flow*, ASME, 1-10 (1978).

Herman, G. T., A. Lent, and S. W. Rowland, "ART: Mathematics and Applications," *J. Theor. Biol.*, **42**, 1 (1973).

Hewitt, G. F., and P. C. Lovegrove, "Experimental Methods in Two-Phase Flow Studies," Electric Power Research Institute Report, *EPRI NP-118* (1976).

Petrick, M., and B. S. Swanson, "Radiation Attenuation Method of Measuring Density of a Two-Phase Fluid," *Review of Scientific Instruments*, **29**, No. 12, 1079 (1958).

Zakaib, G. D., A. A. Harms, and J. Vlachopoulos, "Two-Dimensional Void Reconstruction by Neutron Transmission," *Nucl. Sci. and Eng.*, **65**, 145 (1978).

Manuscript received March 10, 1980; revision received July 14, and accepted July 16, 1980.

Efficiency of Mixing from Data on Fast Reactions in Multi-Jet Reactors and Stirred Tanks

J. M. OTTINO

Department of Chemical Engineering and Materials Science
University of Minnesota
Minneapolis, MN 55455

Some fluid mechanical information concerning mixing generation in complex flow fields can be obtained from conversion data of fast chemical reactions. Computation of such information and averages required in the procedure are presented here. Complex turbulent flow fields present deterministic-like behavior when analyzed in average sense with regard to mixing generation.

SCOPE

Mixing with chemical reaction is a process that involves fluid mechanics, diffusion, and kinetics. In general, these three mechanisms govern reaction in any reacting mixture. Any reasonable mixing description should give an emphasis to all of these processes in proportion to the importance of their effects.

The independent variable of mixing of reacting fluids without changes in physical properties is the flow field. Chemical reaction results, such as spatial distributions of conversion or selectivity, are dependent variables governed by fluid mechanical effects. It is then, in principle, possible to obtain fluid

The author is presently with Department of Chemical Engineering, University of Massachusetts, Amherst, MA 01003.